Bull. Mater. Sci., Vol. 39, No. 7, December 2016, pp. 1651–1663. © Indian Academy of Sciences.
DOI 10.1007/s12034-016-1329-1

Characterization of Fe^{3+}-doped silver phosphate glasses

B P CHOUDHARY and N B SINGH*
Research and Technology Development Centre, Sharda University, Greater Noida 201306, India

MS received 30 July 2015; accepted 5 May 2016

Abstract. **The relationship among the composition, structure and selected properties for five series of silver phosphate glasses containing 0, 5, 10, 15 and 20 wt% Fe_2O_3 has been investigated. The synthesized glasses have been characterized using different experimental techniques. X-ray diffraction studies revealed that the glasses are amorphous in nature. IR spectral studies have shown the presence of characteristic P–O–P linkages of linear phosphate chains, presence of O–P–O units in the phosphate tetrahedral and the formation of P–O–Fe bonds in the doped glass. It is also confirmed that due to doping of Fe_2O_3, loosening of glassy structure occurred and the glass became more disordered. Differential scanning calorimetric (DSC) studies revealed that glass transition temperature increased with Fe_2O_3 concentration. Scanning electron microscopic studies have shown that Fe_2O_3 doping modifies the microstructures of the glass and at lower concentration of dopant, a nanostructure is obtained. Electrical conductivity measurements from 303 to 373 K in a frequency range from 100 Hz to 5 MHz have indicated that all glasses are ionic conductors with Ag^+ ions as the charge carrier. Fe_2O_3 doping in silver phosphate glass increased the electrical conductivities. Results have shown that dielectric constants increased with the increase of temperature at all the frequencies; a.c. and d.c. conductivities have been separated and a Cole–Cole plot is also drawn. Dielectric losses in all the glasses decreased with frequency at a particular temperature. It is found that Ag_2O–P_2O_5 glass doped with 5 wt% Fe_2O_3 gives high OCV value and the doped glass can be used as an electrolyte for solid-state batteries.**

Keywords. **Doping; glasses; FTIR; ionic conductivities; XRD.**

1. Introduction

During the past years phosphate-based glasses have been found for a variety of applications due to their several special properties such as large thermal expansion coefficients, low melting temperatures, solubility, etc. [1]. The properties that make phosphate glasses candidates for so many different applications are related to their molecular level structures [2]. However, practical applications of phosphate glasses are limited because of their chemical durability but this can be enhanced considerably by using suitable dopants. One of the striking features of ion-conducting glasses is compositional dependence of the conductivity. Most of the ion-conducting glasses studied so far consist of three components, such as a glass former, metal oxide acting as a network modifier and metal halide/oxide acting as a dopant. The usual way to increase the conductivity of these glasses is to increase the modifier or dopant content [3]. In recent years, considerable amount of research work has been carried out on solid-state batteries using superionic solids as electrolytes. Silver-ion-conducting glasses (superionic solids) exhibit high electrical conductivity and therefore they are attractive as electrolytes for all-solid-state batteries or microbatteries operating at ambient temperature [4–6]. Recently, we used BaO/SrO as dopants in silver phosphate glass and studied various properties [7,8]. Attempts were made to understand properties of the glasses. It is reported that nanosize dopants modify the properties to a great extent. When silver phosphate glasses are doped with Fe_2O_3, nanostructural glass is obtained and it is expected that there will be considerable change in properties [9]. In this paper, attempts have been made to understand the structure–property relationship in silver phosphate glass doped with 0, 5, 10, 15 and 20 wt% Fe_2O_3 in the temperature range of 303–373 K and a frequency range of 100 Hz–5 MHz.

2. Materials and methods

2.1 *Materials*

All the chemicals used in the preparation of silver phosphate glass were of analytical grade. $AgNO_3$, ammonium dihydrogen phosphate, ferric acetate and NaOH pallets were used as such without any further purification.

2.2 *Preparation of iron oxide*

In a typical procedure, a known weight of ferric acetate was dissolved in distilled water and stirred for half an hour. Dilute NaOH solution was added drop by drop for 4 h, where ferric hydroxide was precipitated and agglomeration was avoided. After that the precipitate was kept overnight and then filtered, washed with hot water several times and dried in a hot air oven at 80°C for 12 h. The dried sample was heated at 500°C, where Fe_2O_3 was obtained.

*Author for correspondence (nbsingh43@gmail.com)

2.3 *Preparation of glasses*

Melt quench technique was employed to prepare the glasses [7–10]. Undoped silver phosphate glass was prepared by heating a 1:1 molar mixture of silver nitrate and ammonium dihydrogen phosphate in a platinum crucible. Similarly, for preparing silver phosphate glass doped with 5, 10, 15 and 20 wt% Fe_2O_3, appropriate amount of freshly prepared Fe_2O_3 was added to a 1:1 molar mixture of silver nitrate and ammonium dihydrogen phosphate in platinum crucibles. In all the cases, the mixtures were first heated slowly in an oven at 150–200°C till the evolution of gases ceased. Proper care was taken that the material did not spurt out from the crucible in the initial stages when the frothing took place. These mixtures were then finally heated in an electric muffle furnace at 800–900°C for 1–2 h and the melts were then suddenly quenched at 0°C to form glassy products. These glasses were then dried in an oven at 100°C, stored in sample tubes and kept in a desiccator.

2.4 *X-ray diffraction studies*

X-ray diffraction patterns of all the samples of doped and undoped silver phosphate glasses were recorded with an X-ray powder diffractometer using Cu K_α radiation.

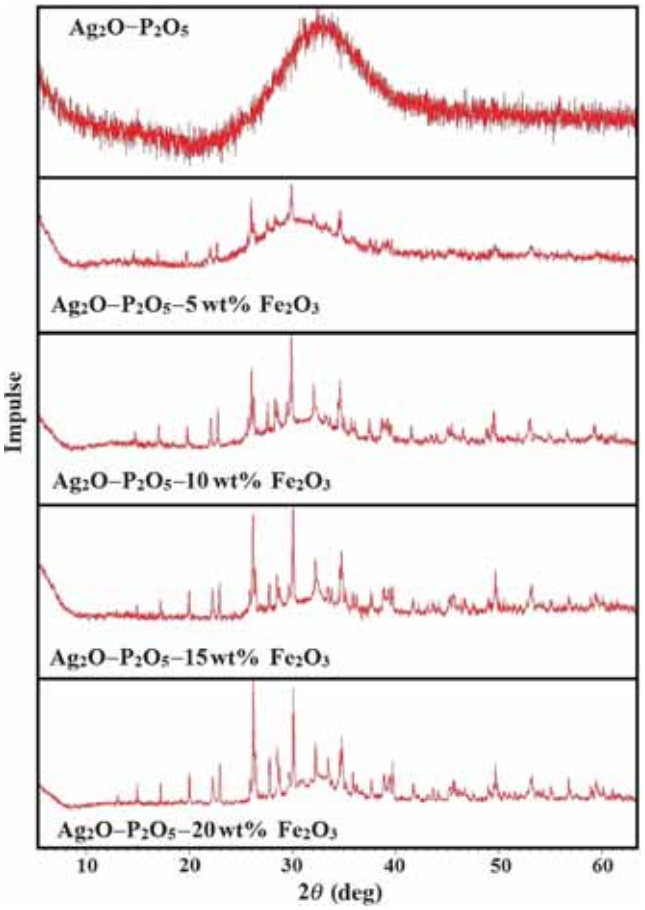

Figure 1. X-ray diffraction patterns of undoped and doped silver phosphate glasses.

2.5 *FT-IR spectral studies*

FT-IR spectra of the glasses were recorded with the help of a Shimadzu IR AFFINITY-1 spectrometer at room temperature in the range of 2000–400 cm^{-1} using KBr pellets.

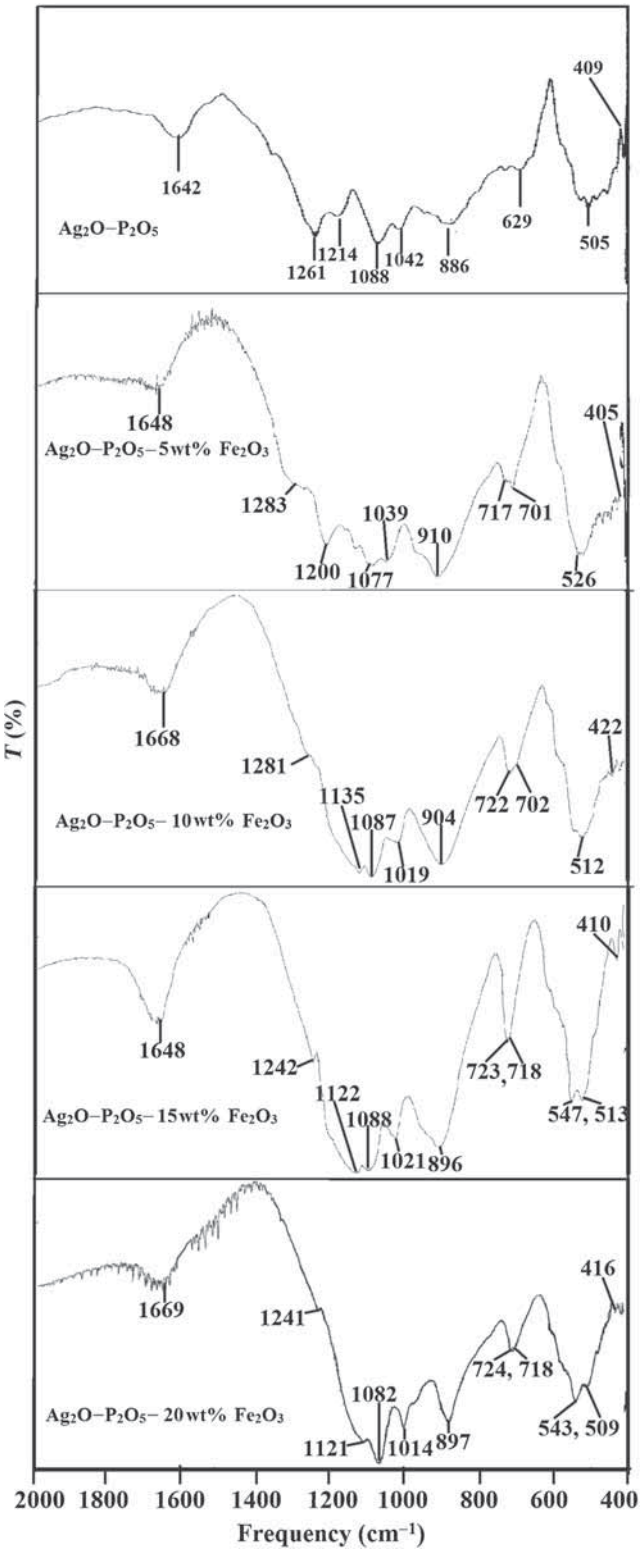

Figure 2. Infrared spectra of undoped and doped silver phosphate glasses.

2.6 *Scanning electron microscopic (SEM) studies*

ESEM studies of glasses were carried out with a Quanta FEG 250 ESEM.

2.7 *Differential scanning calorimetric (DSC) studies*

DSC studies of undoped Ag_2O–P_2O_5 and Fe_2O_3-doped Ag_2O–P_2O_5 glasses were carried out with the help of a METTLER TOLEDO DSC 822e instrument at a heating rate of 10°C min^{-1} in nitrogen atmosphere.

2.8 *Electrical conductivity measurements*

The electrical conductivities of undoped and doped silver phosphate glasses were measured by the a.c. impedance spectroscopic method using a HIOKI 3532-50 LCR Hi TESTER. Pellets of the glass samples were made with the help of a hydraulic press machine in a die by applying a pressure of 5 tonnes. The pellets were coated with silver paste on both the sides and kept between two electrodes (two-probe method). The sample holder was kept in a furnace and the conductivity measurements were carried out in the temperature range of 303–373 K at different frequencies ranging from 100 Hz to 5 MHz. From the measurements, dielectric constants and dielectric losses were also evaluated.

2.9 *Fabrication of battery*

Four batteries were fabricated using silver metal as the anode [11]. The Ag_2O–P_2O_5 and 5%-Fe_2O_3-doped Ag_2O–P_2O_5 glasses were powdered and pressed in a pelletizing die to give the desired electrolyte pellets. A mixture of graphite and iodine in 1:1 weight ratio was used as the cathode. The materials used for the cathode were ground into fine powders, mixed, transferred to the die and pressed into a pellet. In all the cases, a pressure of 5 tonnes cm^{-2} was applied to produce pellets of electrolytes and cathode. The electrolyte pellet's dimensions (diameter 0.76 cm and thickness 0.50 cm) were kept the same in each case. The electrolyte pellet was kept between the cathode pellet and the silver metal anode in a sample holder to give the desired batteries. For characterizing the cells, the OCVs and discharge characteristics were monitored at room temperature (30°C) with a humidity level of 40%. The OCVs of all the cells were measured immediately after their fabrication by means of a digital multimeter. The discharge characteristics of all the cells were monitored under a constant load of 100 kΩ. For the same load resistance, the voltage (V) was measured as a function of time in a way similar to that as reported earlier [12].

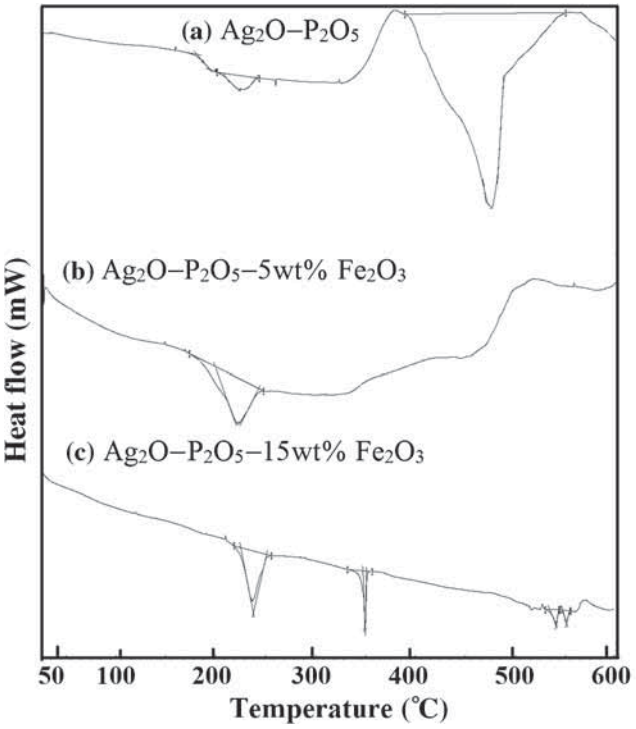

Figure 3. DSC thermographs of undoped and doped silver phosphate glasses.

Table 1. Infrared absorption frequencies of undoped and doped glasses in the range 2000–400 cm^{-1}.

Vibration modes	Frequency for Ag-PO_4	Frequency for Ag-PO_4–5% Fe_2O_3	Frequency for Ag-PO_4–10% Fe_2O_3	Frequency for Ag-PO_4–15% Fe_2O_3	Frequency for Ag-PO_4–20% Fe_2O_3
Bending vibration of O–P–O bonds	409, 505	405, 528	422, 512	410, 513, 547	416, 509, 543
Symmetric stretching vibration of P–O–P linkage	629	701, 717	702, 722	718, 723	718, 724
Asymmetric stretching vibration of P–O–P linkage	886	910	904	896	897
Vibration modes of PO_3^{4-} group	1042	1039	1019	1021	1014
Asymmetric stretching modes of chain terminating at PO_3^{2-}	1088, 1214	1077, 1200	1087, 1135	1088, 1122	1082, 1121
Asymmetric stretching of double bonded P=O modes	1261	1283	1281	1242	1262
Bending vibration modes of O–H group in H–O–H modes	1642	1648	1668	1648	1669

3. Results and discussion

The X-ray diffraction patterns of all the undoped and Fe^{3+}-doped Ag_2O–P_2O_5 glasses are shown in figure 1. Undoped silver phosphate glass is very poorly crystalline or amorphous in nature. However with increasing amount of Fe^{3+} dopant, crystallinity of the glass increased. This may be due to modifications in the glassy structure.

Table 2. Glass transition temperature.

Material	Glass transition temperature (°C)
Ag_2O–P_2O_5	180.96
Ag_2O–P_2O_5–5 wt% Fe_2O_3	197.57
Ag_2O–P_2O_5–15 wt% Fe_2O_3	226.15

FT-IR spectra of doped and undoped silver phosphate glasses are shown in figure 2. The assignments of vibrational bands are given in table 1. The spectra of undoped Ag_2O–P_2O_5 glass exhibit the characteristic bands at 409, 505, 629, 886, 1042, 1088, 1214, 1261 and 1652 cm^{-1}. The spectral bands appearing at 409 and 505 cm^{-1} could be assigned to the bending vibrations of O–P–O and O=P–O units [7]. The two absorption bands appearing at 629 cm^{-1} is due to the symmetric stretching modes of P–O–P linkages, while the band appearing at 886 cm^{-1} could be assigned to the asymmetric stretching mode of P–O–P linkages [7]. These bands indicate the presence of a linear metaphosphate (P–O–P) chain in the silver phosphate glass. The spectral bands appearing at ∼1042 and ∼1088 cm^{-1} have been assigned to $P–O^-$ groups, i.e., vibrational modes of PO_4^{3-} group and asymmetric stretching modes of chain terminating at $(PO_3)^{2-}$,

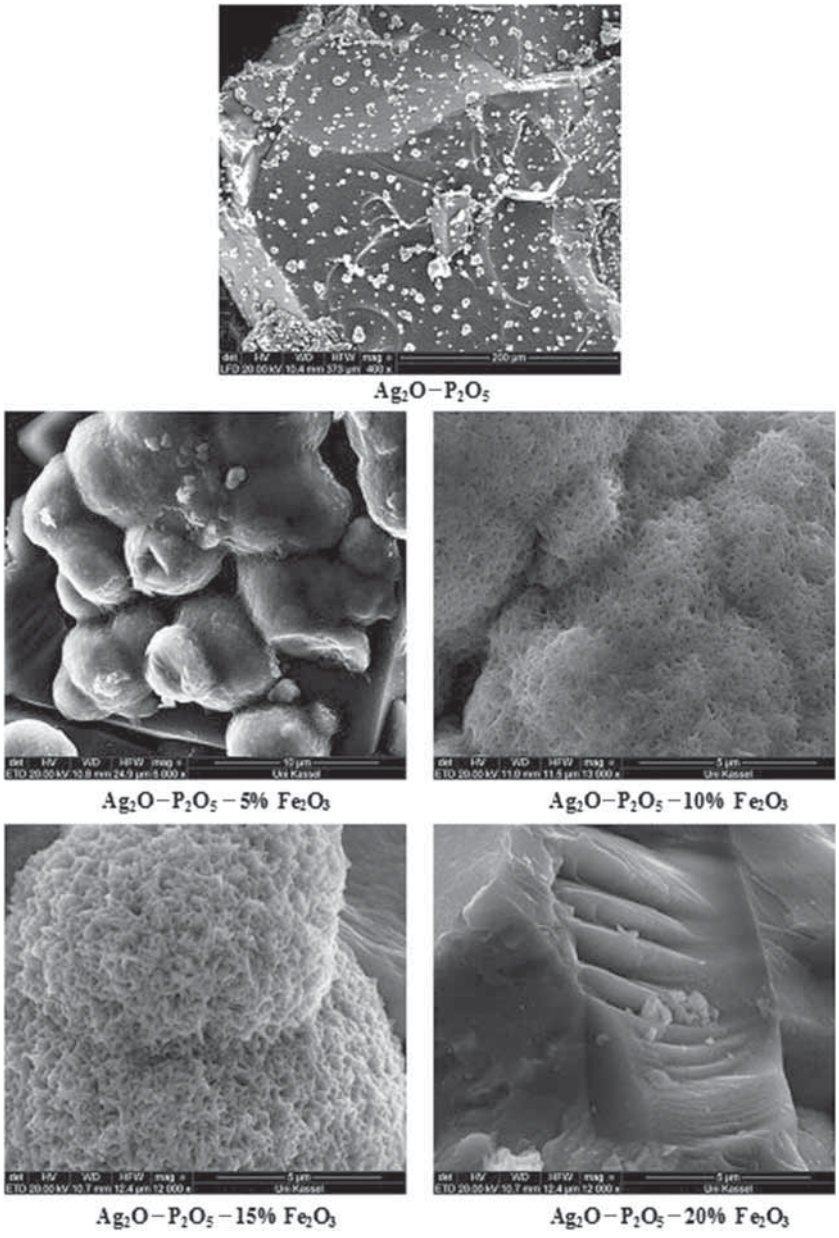

Figure 4. SEM images of undoped and doped silver phosphate glasses.

respectively. The strong band appearing at 1261 cm^{-1} is ascribed to asymmetric stretching of double bonded P=O modes, i.e., υ_{asy} PO_2 in the phosphate tetrahedra. The strong band at 1652 cm^{-1} may be attributed to bending modes of O–H groups (P–O–H bridges) and molecular water due to absorption of moisture during KBr pellet preparation. In the presence of Fe_2O_3, different vibrational bands are found to shift. This indicates that the Fe_2O_3 changes the glassy structure of the undoped silver phosphate glass. The observed band appearing at 409 and 505 cm^{-1} in the undoped Ag_2O–P_2O_5 glass was found to shift to higher frequency in doped glass. The observed bands at 629 cm^{-1} in undoped Ag_2O–P_2O_5 glass get broadened and shifted to higher frequencies in the presence of Fe_2O_3. The observed bands at 1042 cm^{-1} in undoped Ag_2O–P_2O_5 glass get shifted to lower frequencies in the presence of Fe_2O_3. The observed band at 1214 cm^{-1} in undoped Ag_2O–P_2O_5 glass gets shifted to lower frequencies in the presence of Fe_2O_3. The band observed at 1261 cm^{-1} in undoped glass remained unchanged in doped Ag_2O–P_2O_5 glasses. The observed bands at 1652 cm^{-1} in undoped Ag_2O–P_2O_5 glass gets shifted in the presence of Fe_2O_3. On the basis of FTIR spectra it can be inferred that on the addition of Fe_2O_3, the basic structure of Ag_2O–P_2O_5 glass is almost the same but some P–O–Ag bonds present in the undoped Ag_2O–P_2O_5 glass may be replaced by P–O–Fe_2O_3 bonds. It could be proposed that Fe^{3+} ions get attached to the negative end of the P–O^- ….Ag^+ bond of the undoped glass and replace the Ag^+ ions. Thus the dopant metal ions form a P–O^- ….Fe^{3+} bond in the glass structure and Fe^{3+} ions serve as ionic cross-links between the non-bridging oxygen of two different phosphate chains. However, the P–O–P bonds in the glass network are not affected. Since the size of Fe^{3+} (63 pm) is lower than that of Ag^+ (129 pm), incorporation of Fe^{3+} in glass may create a loosening of the glass structure.

DSC curves of silver phosphate glasses are given in figure 3. The glass transition temperature (T_g) of Ag_2O–P_2O_5 and Fe_2O_3-doped Ag_2O–P_2O_5 glasses were determined from DSC curves and are given in table 2. The glass transition temperature for Ag_2O–P_2O_5 is found to be 180.96°C. In the presence of 5-wt% Fe_2O_3 and 15-wt% Fe_2O_3, the glass transition temperatures are shifted to higher temperatures, i.e., 197.57 and 226.15°C, respectively. Further, in doped glasses, the melting temperatures are not sharp and a broad endothermic peak at about 450°C is obtained. The decrease in the sharpness of this peak suggests that Fe_2O_3-doped glass is less crystalline. The higher T_g values of the doped glass suggest an increase in the cross-link density, which improves its chemical durability.

The increase of glass transition temperature generally depends on the chain length of the phosphate glasses, cross-link density and nature of bonding. It has been reported that the ultraphosphate glasses consist of 3D cross-linked network, which increases T_g. However, the dependence of T_g on dopant is quite complex. This complex behaviour of glass transition temperature has been attributed to the cation–polyanion (PO_3) interaction, which governs the polyanions mobility. When Fe_2O_3 is doped in the phosphate network, P–O–Fe bonds are formed. Strength of the bond depends on the behaviour of Fe^{3+} cations, i.e., it acts both as a network former and as a network modifier.

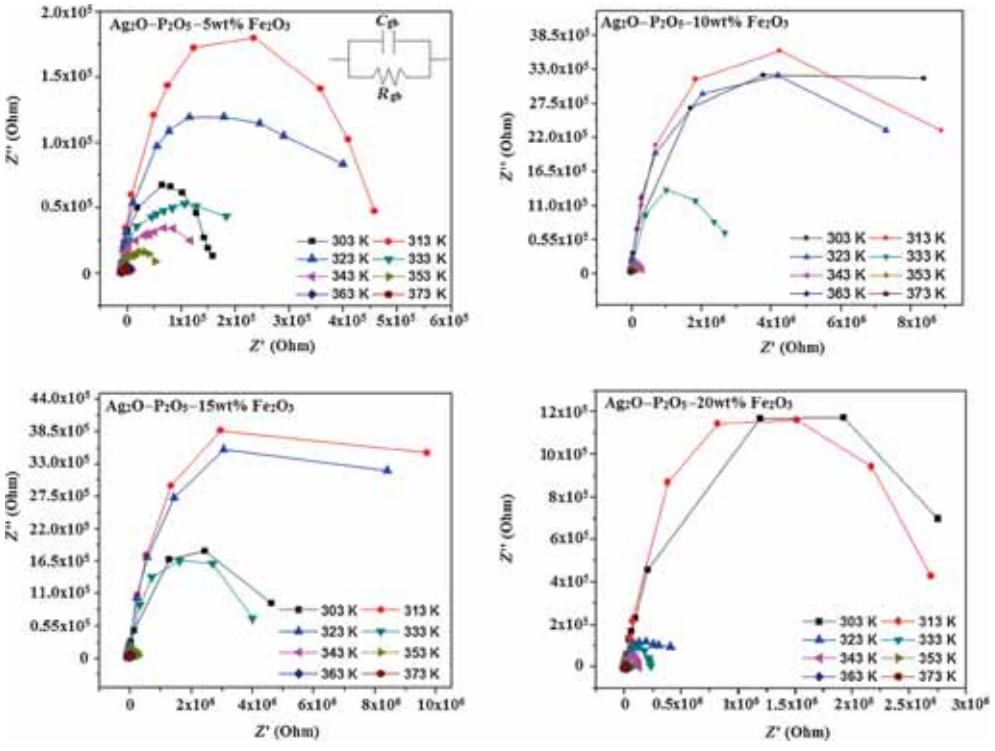

Figure 5. Cole–Cole plot for electrical conductivity.

Scanning electron microscopic (SEM) images are shown in figure 4. SEM of undoped silver phosphate shows plate-like structure with small particles on the surface. In the presence of Fe_2O_3, morphologies changed. In the presence of 5.0 wt% concentration Fe_2O_3, nanosize symmetrical nodular particles with a neck (34 nm) are formed. In the presence of 10 wt% Fe_2O_3, spongy particles with nanopores are formed. With further addition of Fe_2O_3 (15 wt%) the spongy structure is retained but the pores become micro-sized. However, in the presence of 20 wt% Fe_2O_3, morphology is completely changed and fractured surfaces are obtained. The results clearly indicate that Fe_2O_3 doping changes the morphology of silver phosphate glass and at lower concentration nanodimensional glassy structure is obtained.

In order to investigate the electric transport mechanism in the glasses the complex impedance Cole–Cole (Z'–Z'') plots of Fe_2O_3-doped silver phosphate glasses for several

Table 3. List of the values of $\sigma_{d.c.}$ and $\sigma_{a.c.}$ at 373 K.

Glass	$\sigma_{d.c.}$ (S cm^{-1})	$\sigma_{a.c.}$ (S cm^{-1})	S
Ag_2O–P_2O_5	1.14E–5	9.70E–6	0.06
5% Fe_2O_3–Ag_2O–P_2O_5	6.23E–5	1.19E–5	0.13
10% Fe_2O_3–Ag_2O–P_2O_5	8.25E–6	7.71E–6	0.12
15% Fe_2O_3–Ag_2O–P_2O_5	5.71E–6	1.97E–6	0.17
20% Fe_2O_3–Ag_2O–P_2O_5	2.32E–5	1.12E–5	0.10

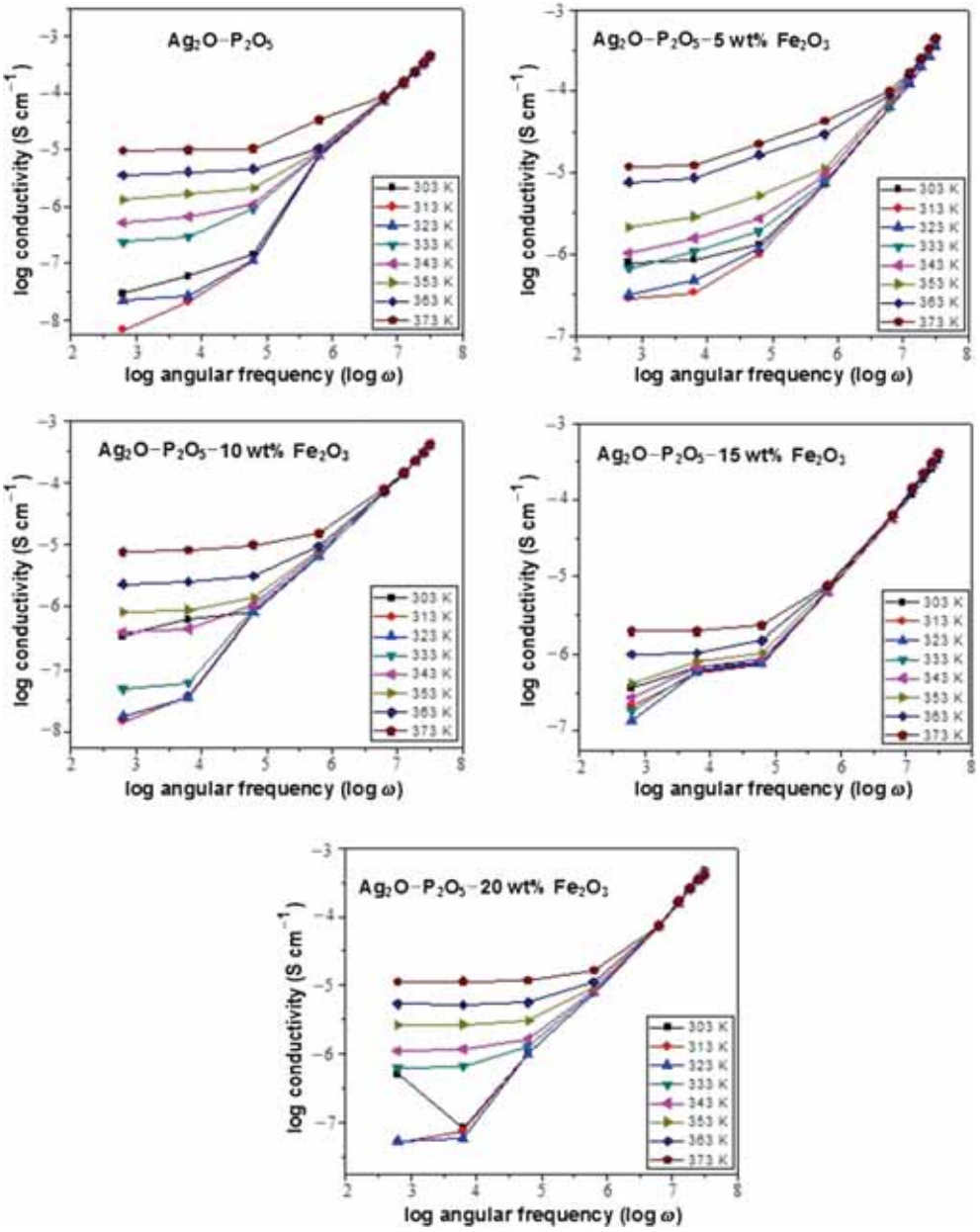

Figure 6. Variation of log conductivity with log angular frequency (Almond–West plot).

Table 4. Change in conductivities of undoped and doped glasses.

Glass	Frequency (kHz)	Conductivity 303 K	Conductivity 373 K	Dielectric constant 303 K	Dielectric constant 373 K	Dielectric loss 303 K	Dielectric loss 373 K
Ag_2O–P_2O_5	0.1	2.91E–8	9.70E–6	267	2780	1.862	9.999
	1.0	5.87E–8	9.99E–6	201	2340	1.051	9.999
	10	1.43E–7	1.05E–5	224	628	0.374	6.384
5% Fe_2O_3–Ag_2O–P_2O_5	0.1	7.94E–7	1.19E–5	10500	195000	4.117	9.999
	1.0	8.59E–7	1.25E–5	2640	54500	2.353	4.001
	10	1.33E–6	2.29E–5	1580	20800	0.397	2.216
10% Fe_2O_3–Ag_2O–P_2O_5	0.1	$3.47E^{-7}$	7.71E–6	1040	74700	2.344	9.999
	1.0	$6.19E^{-7}$	8.29E–6	636	13000	0.633	9.999
	10	$8.21E^{-7}$	9.81E–6	1440	3440	0.221	5.022
15% Fe_2O_3–Ag_2O–P_2O_5	0.1	$3.65E^{-7}$	1.97E–6	1150	7570	4.019	9.999
	1.0	$6.65E^{-7}$	1.96E–6	815	2390	0.745	9.999
	10	$8.06E^{-7}$	2.34E–6	1400	1710	0.266	2.250
20% Fe_2O_3–Ag_2O–P_2O_5	0.1	$5.01E^{-7}$	1.12E–5	1620	24200	5.320	9.999
	1.0	$8.29E^{-7}$	1.14E–5	1030	4620	0.994	9.999
	10	$1.02E^{-6}$	1.19E–5	1700	2430	0.321	8.525

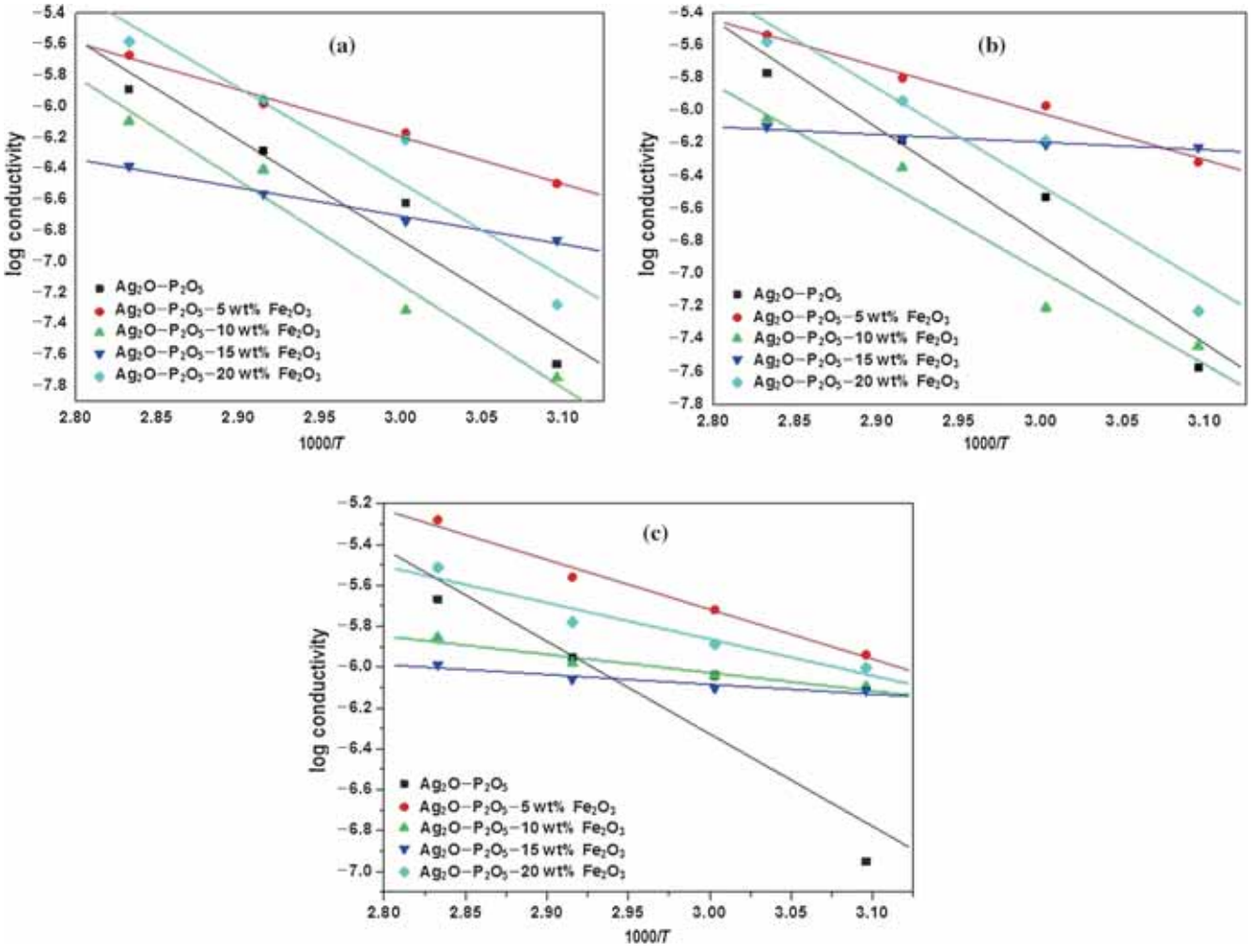

Figure 7. Arrhenius plot of electrical conductivity of undoped and Fe_2O_3-doped Ag_2O–P_2O_5 glasses at frequencies **(a)** 0.1, **(b)** 1 and **(c)** 10 kHz.

temperatures are made (figure 5). It is found that all the studied glasses exhibit similar behaviour and the plots show a single semicircle, indicating a single relaxation process with different relaxation times. With the increase of temperature, the area under the semicircle of Cole–Cole plots is decreased, indicating the tendency of better conductivity. Thangadurai *et al* [13] have pointed out that if there is one circle, it may possess one type of conducting behaviour and according to Santic *et al* [14] the single impedance arc is typical of electronic conduction. Thus in the temperature range studied, the electronic conductivities may be the dominant mechanism of conduction.

It is reported that transition-metal-oxide-doped glasses show mixed electronic–ionic conduction. When Fe_2O_3 is doped in silver phosphate glass, both Fe^{2+} and Fe^{3+} ions may be present and will play diverse roles in the conduction process. The P–O–Fe bonds are believed to be replaced either by P–O–Fe^{3+} or P–O–Fe^{2+} bonds. The electronic conduction in Fe_2O_3-doped glass is possible by the electron transfer from Fe^{2+} to Fe^{3+} ions. The electronic conduction may take place by polaron hopping between Fe^{3+} and Fe^{2+} and the ionic conduction comes up from Fe^{3+} dispersion in glass. It is observed that the conductivities increased with increasing frequencies and temperatures in all the cases. This may be due to low-frequency dispersion, high frequency dispersion and electrode polarization [15,16]. Electrical conductivities of all the glasses were measured at different temperatures (303–373 K) and at different frequencies (100 Hz–5 MHz). The variation of electrical conductivity is shown by the Almond–West power law (figure 6)

$$\sigma_{\text{a.c.}} = \sigma_0 + A\omega^S, \tag{1}$$

where σ_0 is the d.c. conductivity (conductivity at zero frequency) and ω is angular frequency ($\omega = 2\pi f$); A and S are power-law-fit parameters. The comparative values of d.c. conductivity and a.c. conductivity at 373 K are tabulated in table 3. The variation of log $\sigma_{\text{a.c.}}$ with log of angular frequency (log ω) at different temperatures is shown in figure 6. At a particular temperature the a.c. conductivity patterns show a frequency-independent plateau in the low-frequency region and exhibit sudden increase at the higher frequencies. The values of the electrical conductivity of undoped and doped Ag_2O–P_2O_5 glasses at different frequencies and at two different temperatures are also given in table 4. From table 4 it is clear that as the frequency and temperature increased, the σ-values of all the samples increased. It is observed that the conductivities of the undoped Ag_2O–P_2O_5 glass are lower than those of the Fe_2O_3-doped silver phosphate glass at all frequencies and temperatures. Higher frequencies increase the loosening of the glass network and as a result, ionic mobility increases. This leads to increase in conductivity. The nature of variation of $\sigma_{\text{a.c.}}$ follows the universal dynamic response [17]. According to the jump relaxation model [18], at very low frequencies ($\omega \rightarrow 0$) an ion can jump from one site to its neighbouring vacant site successfully, contributing to the d.c. conductivity. At higher frequencies, the probability for the ion to go back again to its initial site increases due to the short time periods available. This high probability for the correlated forward–backward hopping at higher frequencies together with the relaxation of the dynamic cage potential is responsible for the observed high-frequency conductivity dispersion. At higher frequencies, the electrical signal gives excitation energy to the charge carriers, which in turn increases the mobility of the charge carriers and decreases the relaxation time. Hence, an increase in conductivity is noticed with increasing frequencies.

Further, in the undoped glass, probably the number of Ag^+ ions is not sufficient to move in the glassy network. However, on doping with Fe_2O_3, the conductivity increases to a great extent (table 4). The dopant metal ions lead to an increase in the number of mobile Ag^+ ions in the glass network

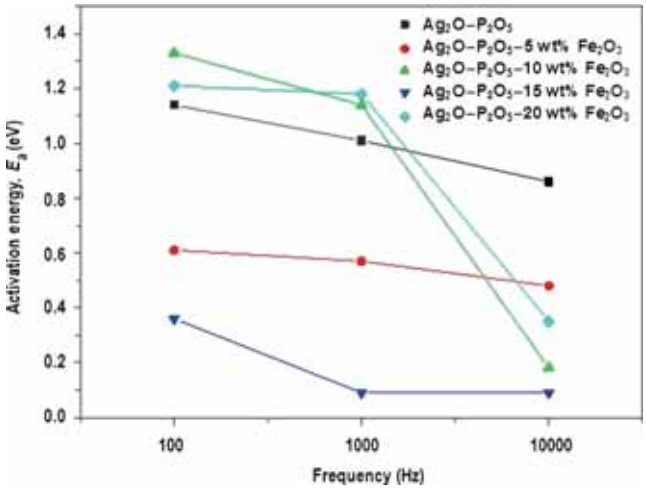

Figure 8. Variation of energy of activation with frequency.

Table 5. Energy of activation of undoped and doped glasses.

Frequency (Hz)	E_a Ag_2O–P_2O_5 (eV)	E_a 5% Fe_2O_3–Ag_2O–P_2O_5 (eV)	E_a 10% Fe_2O_3–Ag_2O–P_2O_5 (eV)	E_a 15% Fe_2O_3–Ag_2O–P_2O_5 (eV)	E_a 20% Fe_2O_3–Ag_2O–P_2O_5 (eV)
100	1.14	0.61	1.33	0.36	1.21
1000	1.01	0.57	1.14	0.09	1.18
10000	0.86	0.48	0.18	0.09	0.35

and hence an increase in conductivity is noticed. FTIR studies suggest that in the doped Ag_2O–P_2O_5 glass P–O^-–Ag^+ bonds exist [7]. When Fe_2O_3 is introduced, some of the Ag^+ ions get replaced by Fe^{3+} ions during glass formation and P–O–Fe^{3+} bonds are formed between two different chains of silver phosphate glass. These replaced Ag^+ ions in the glass network are responsible for an increase in σ values of the doped glasses. Also some of the free Fe^{3+} ions may be responsible for increased conductivities.

Plots of $\log(\sigma)$ with reciprocal of temperature (323–353 K) at different frequencies gave straight lines (figure 7), showing the validity of Arrhenius equation

$$\sigma = A \exp(-E_a/kT), \tag{2}$$

where E_a is the activation energy for conduction, A is a pre-exponential factor and k is the Boltzmann constant. Table 5 gives the values of E_a. The values decreased with increase of frequency in all the cases. However, there is no definite

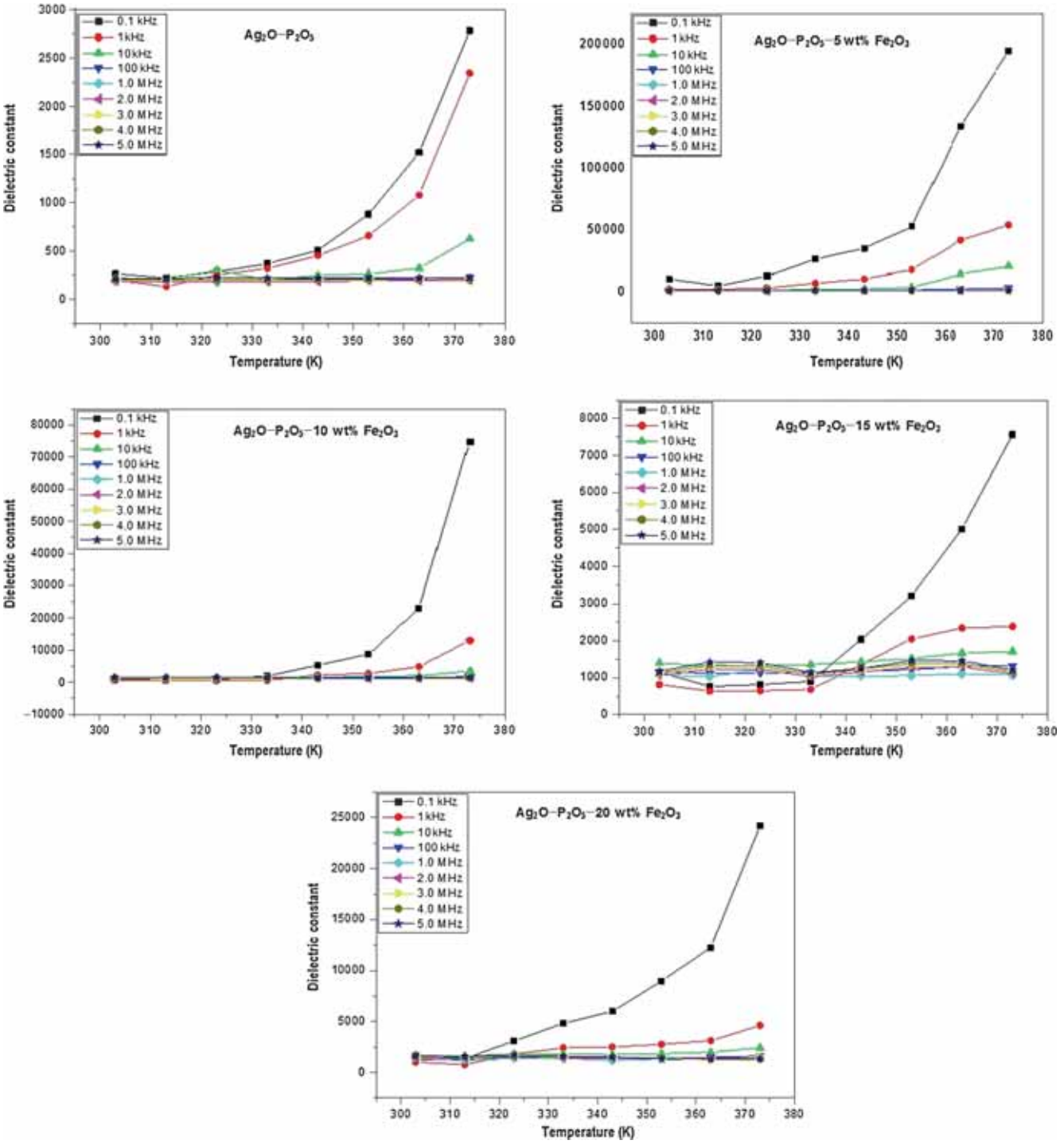

Figure 9. Variation of dielectric constant of undoped and Fe_2O_3-doped silver phosphate glasses with temperature at different frequencies.

sequence with the increase of Fe_2O_3 concentration. It is already reported that upon doping and increasing the temperature loosening of the glassy network occurs [7], which facilitates the easy migration of mobile Ag^+ ions in the glass matrix. The energy of activation is minimum in the case of 15.0-wt%-Fe_2O_3-doped glass. Similar observations are made when energy of activation is plotted against frequency (figure 8). It appears that probably 15 wt% is the most appropriate concentration for Fe_2O_3 doping.

The variations of dielectric constant with temperature at different frequencies in undoped and doped Ag_2O–P_2O_5 glasses are shown in figure 9. Results show that dielectric constant increases with the increase of temperature at all frequencies. However, the effect is more pronounced at lower

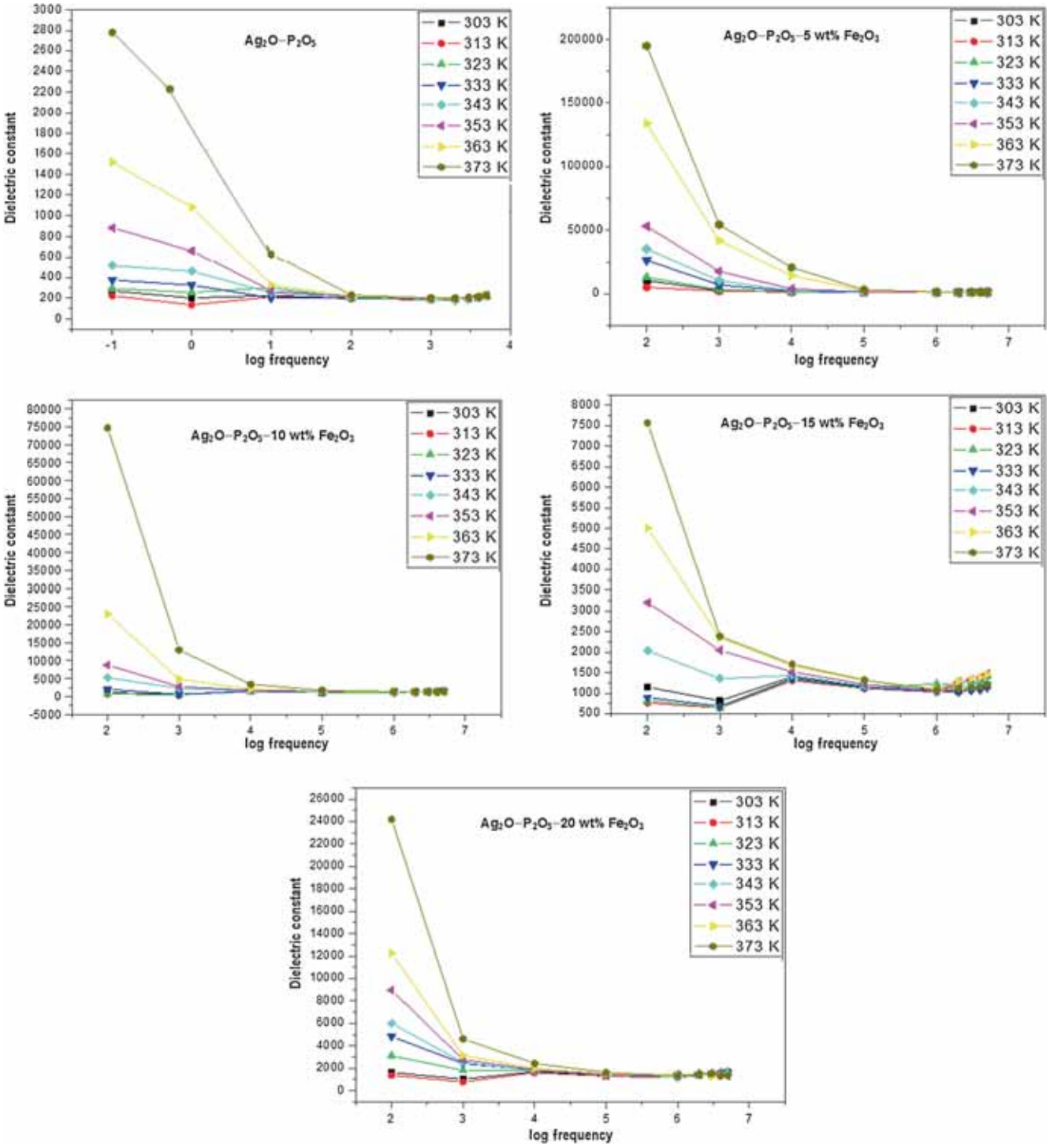

Figure 10. Variation of dielectric constant of undoped and Fe_2O_3-doped silver phosphate glasses with frequency at different temperatures.

frequencies. The increase in dielectric constant with temperature (figure 9) is due to greater freedom of movement of ions at higher temperature.

The dielectric constant decreases with increasing frequency at a given temperature (figure 10). The results have shown that in glasses dipoles exist, corresponding to polaron hopping between sites of different energies. Dielectric constant for a polar material at low frequencies is due to the contribution of electronic, ionic, orientation and space charge polarizations. The total polarization is the sum of all types of polarizations [7]. When the applied field frequency is increased the dipoles are not able to rotate rapidly, so that

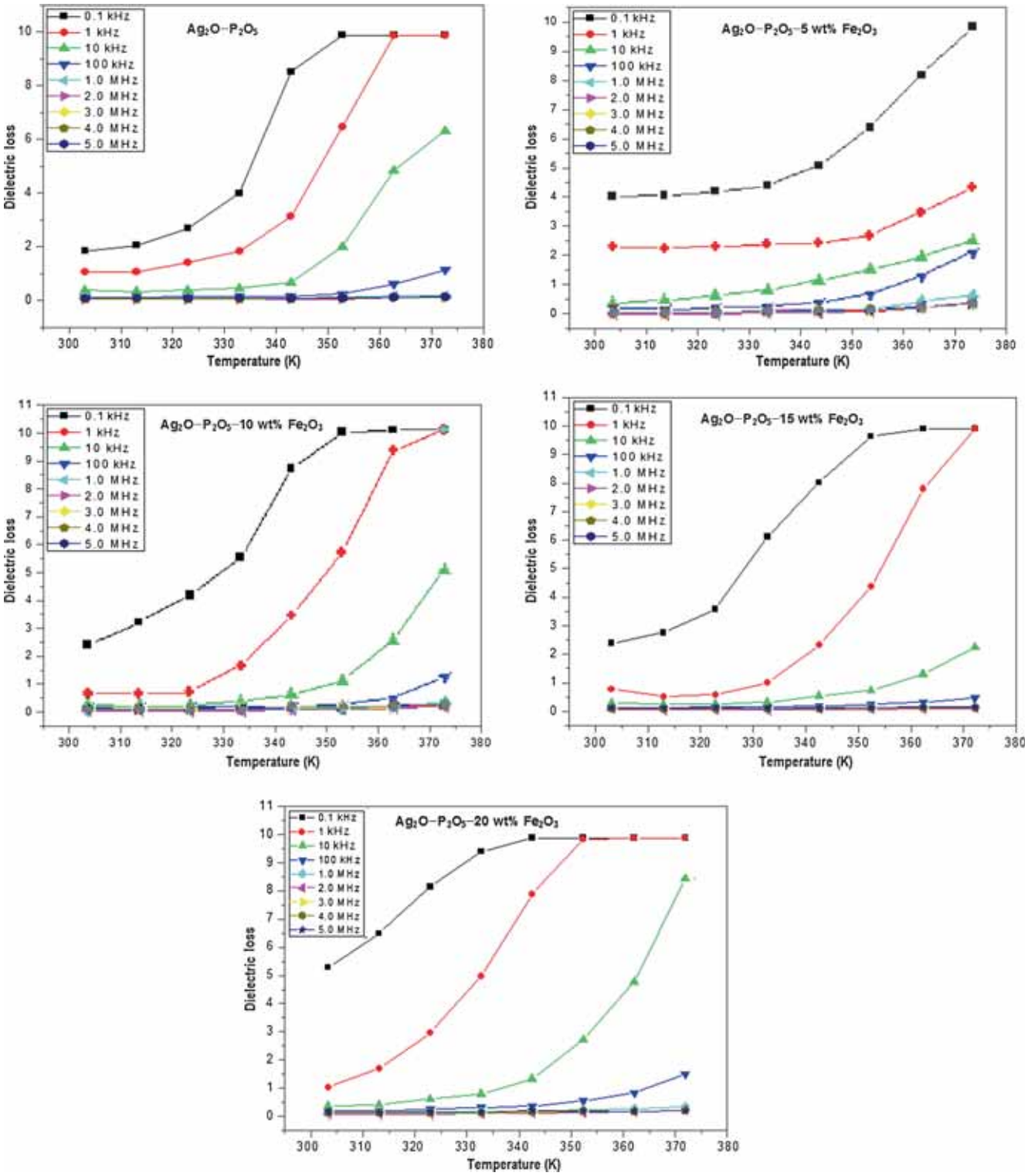

Figure 11. Variation of dielectric loss of undoped and Fe_2O_3-doped silver phosphate glasses with temperature at different frequencies.

their oscillations begin to lag behind those of the applied field. With a further increase in frequency the dipoles are totally unable to follow the field and hence the orientation polarization stops. As a result, the dielectric constant decreases, approaching a constant value due to space charge polarization.

Figure 11 shows the variation of dielectric loss factor with temperature at different frequencies for all the samples. The dielectric loss factor increases with temperature, particularly at lower frequencies. At high frequencies, however, the dielectric loss factor is low and remains more or less constant

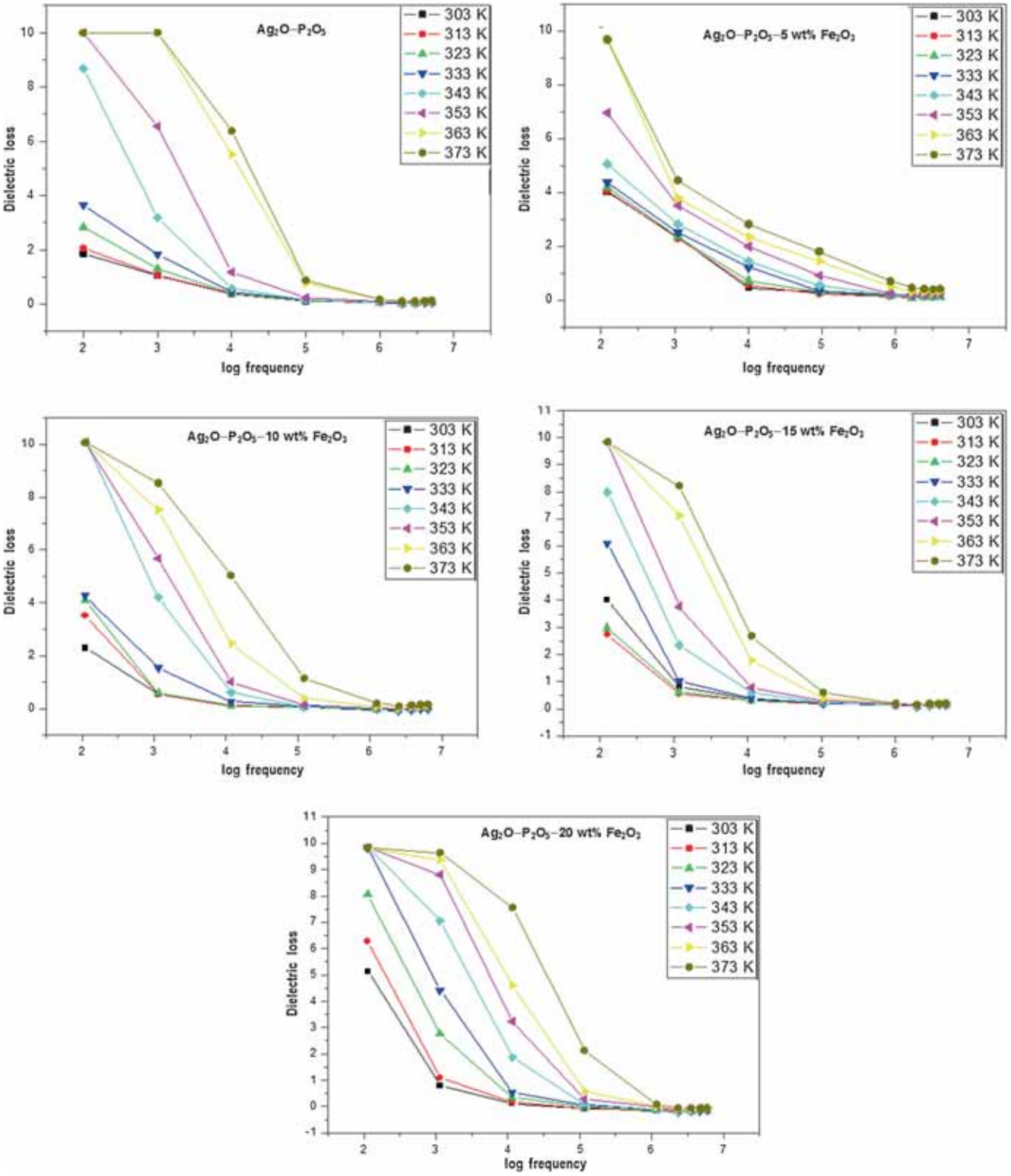

Figure 12. Variation of dielectric loss of undoped and Fe_2O_3-doped silver phosphate glasses with frequency at different temperatures.

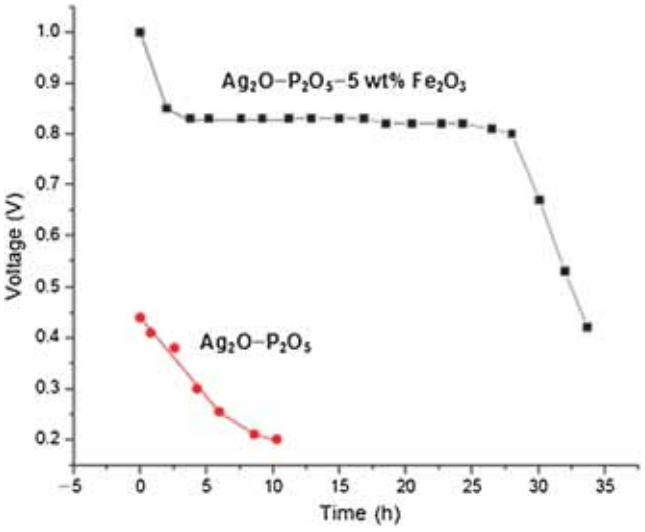

Figure 13. Discharge curves (voltage *vs.* time) at load resistance 100 kΩ: Ag_2O–P_2O_5 and Fe_2O_3-doped Ag_2O–P_2O_5 glass.

with increasing temperature. It appears that the orientation polarization may not keep phase with the rapidly oscillating electric field.

Figure 12 shows the variation of dielectric loss factor with frequency at different temperatures for all the samples. The value of dielectric loss decreases with the increase of frequency at a particular temperature in all the samples.

The variation of voltage with time of the batteries using Ag_2O–P_2O_5 and 5%-Fe_2O_3-doped Ag_2O–P_2O_5 solid electrolyte is shown in figure 13. It is found that OCV value of the solid-state battery using Ag_2O–P_2O_5 is very low. However the OCV value enhances to a large extent when Ag_2O–P_2O_5 glass doped with 5% Fe_2O_3 is used as an electrolyte. This may be due to a nanostructure in the matrix. Also the discharge time of the cell containing 5%-Fe_2O_3-doped Ag_2O–P_2O_5 glass is much higher than that of the cell using Ag_2O–P_2O_5 glass alone.

4. Conclusions

Pure silver phosphate glass and glasses doped with 5.0 wt% Fe_2O_3 were prepared by the quench-melt method. It was found that silver phosphate glass was poorly crystalline in nature but the crystalline character increased with dopant concentration. IR spectral studies have shown the presence of characteristic P–O–P linkages of linear phosphate chains, presence of O–P–O units in the phosphate tetrahedral and the formation of P–O–Fe bonds in the doped glass. DSC studies have shown that glass transition temperature increased with dopant concentration. This indicated an increase in cross-link density. SEM studies have revealed that the morphology of Ag_2O–P_2O_5 glass is changed in the presence of Fe_2O_3. The electrical conductivity increased with temperature and frequency and the values are higher in Fe_2O_3-doped glass. Higher frequencies increased the loosening of the glass network and as a result, ionic mobility increased. Further, Fe^{2+} ions replaced some of the Ag^+ ions and made the doped glass more conducting. The dielectric constant decreased with frequency. The dielectric loss factor increased with temperature, particularly at lower frequencies. It was found that 5-wt%-Fe_2O_3-doped glass can be a good electrolyte for solid-state batteries.

Acknowledgements

We are grateful to Prof. B Middendorf, University Kassel, Germany, for recording X-ray diffraction and SEM pictures. We acknowledge the financial support in the form of a research project from DRDO, New Delhi.

References

[1] Tiwari B, Dixit A, Kothiyal G P, Pandey M and Deb S K 2007 *BARC Newslett.* **285** 167
[2] Brow R K 2000 *J. Non-Cryst. Solids* **263–264** 1
[3] Garbarczyk J E, Pietrzak T K, Wasiucionek M, Kaleta A, Dorau A and Nowinski J L 2015 *Solid State Ion.* **272** 53
[4] Baia L, Muresan D, Baia M, Popp J and Simon S 2007 *Vibr. Spectrosc.* **43** 313
[5] Kabi S and Ghosh A 2014 *Solid State Ion.* **262** 778
[6] Rao G V and Shashikala H D 2014 *J. Non-Cryst. Solids* **402** 204
[7] Choudhary B P and Singh N B 2014 *Emerg. Mater. Res.* **3** 70
[8] Singh N B and Chaudhary B P 2015 *J. Therm. Anal. Calorim.* **120** 1217
[9] Garbarczyk J E, Wasiucionek M, Jozwiak P, Nowinski J L and Julien C M 2009 *Solid State Ion.* **180** 531
[10] Das S S, Baranwal B P, Gupta C P and Singh P 2005 *Indian J. Eng. Mater. Sci.* **12** 58
[11] Das S S, Baranwal B P, Gupta C P and Singh P 2003 *J. Power Sources* **114** 346
[12] Das S S, Srivastava P K, Singh N P and Srivastava V 2010 *Indian J. Eng. Mater. Sci.* **17** 123
[13] Thangadurai V, Huggins R A and Weppner W 2002 *J. Power Sources* **108** 64
[14] Santic A, Kim C W, Day D E and Mogus-Milankovic A 2010 *J. Non-Cryst. Solids* **356** 2699
[15] Mugoni C, Montorsi M, Siligardi C and Jain H 2014 *J. Non-Cryst. Solids* **383** 137
[16] Almond D P, Hunter C C and West A R 1984 *J. Mater. Sci.* **19** 3236
[17] Jonscher A K 1977 *Nature* **267** 673
[18] Funke K 1993 *Prog. Solid State Chem.* **22** 111